Propagation of Tectonic Waves

Y. Ricard *

Department of Geology and Geophysics, Yale University, New Haven, CT, USA

L. Husson

EAPS, Massachussets Institute of Technology, Cambridge, MA, USA

Y. Ricard, Laboratoire des Sciences de la Terre, UMR5570, Université de Lyon 1, Bat Géode, Villeurbanne, 69622, France. (ricard@ens-lyon.fr)

L. Husson, EAPS, Massachussets Institute of Technology, Cambridge, MA, USA. (lhusson@mit.edu)

*Permanent address: Laboratoire des
Sciences de la Terre, UMR5570, Université de
Lyon 1, Bat Géode, Villeurbanne, 69622,
France.

Mountain building depends on the disequilibrium between boundary stresses, either at the base of the deforming lithosphere or its lateral boundaries, and buoyancy stresses arising form lateral density variations within the lithosphere itself. On the basis of the thin viscous sheet approximation, we propose a model which accounts for both crustal and lithospheric thicknesses variations. The deformation is controlled by the sum of the moments of density anomalies (i.e. density anomalies times depth) of compositional and thermal origins. The transport of the compositional moment is obtained from the continuity equation while the transport of the thermal moment is obtained from the heat equation. The resulting set of equations controls the coupled behavior of the crust and lithosphere. It shows that various type of solutions can exist: unstable, stable and propagating. When propagation occurs, the crustal and the lithospheric thickness variations are out of phase. The tectonic waves propagate with velocities around 5 mm yr^{-1} that increase with the crustal thickness and decrease with the lithospheric viscosity. We discuss these solutions and argue that continents may in large part be in a domain of propagating tectonic waves.

1. Introduction

The fundamental role of crustal thickness variations in the stress balance has been acknowledged since Argand [1924], and almost all tectonic models account for it. The lithosphere is a thermal boundary layer and its lateral thickness variations in time and space during an orogenesis are also associated with density variations. Whereas the crust constantly tends to approach a uniform thickness because it is lighter than the underlying mantle, the cooling lithospheric mantle is denser than the underlying asthenosphere and may become unstable, (*e.g.* [Houseman, 1981; Neil and Houseman, 1999; Conrad, 2000]). The dynamics of orogenesis results from the balance between competiting processes of crustal and lithospheric thickening.

2. The Model

A thin viscous sheet approximation has been extensively used to describe the dynamics of the crust, (*e.g.* [England and McKenzie, 1982; Houseman and England, 1993; Husson and Ricard, 2004]). This approximation is based on the vertical integration of the Navier-Stokes equations, coupled with mass conservation of the crust which controls the time evolution of the model. Lemery et al. [2000] have extended this approach in the case of thermal density variations to derive a boundary layer model of convection at very large Rayleigh number. In the present paper we couple these approaches to take into account both compositional and thermal heterogeneities in the deforming lithosphere.

The main assumption of the thin sheet viscous models is that the vertical variations of the horizontal velocity can be neglected within the lithosphere. This holds when the lithosphere is stiff enough with respect to the underlying asthenosphere and when the deformations occur at wavelengths larger than the lithospheric thickness.

2.1. Stress balance

We assume that the lithosphere behaves like an incompressible viscous fluid of viscosity η and that isostasy holds across the whole lithosphere. If the upper and lower boundaries of the lithosphere are traction free, the horizontal equilibrium equation relates the lateral density variations to the viscous stresses by

$$4L_0 \frac{\partial}{\partial x} \eta \frac{\partial u}{\partial x} = \frac{\partial M}{\partial x}, \tag{1}$$

where u denotes the vertically average velocity and L_0 the uniform averaged thickness of the mechanical lithosphere [Lemery et al., 2000]. The quantity M is the moment of the lithospheric mass anomalies and is written [Artyushkov, 1973; Fleitout and Froidevaux, 1982]

$$M = \int_0^{+\infty} \delta\rho g z \, dz, \tag{2}$$

where $\delta\rho$ is the lateral density variation, g the gravitational acceleration, z the depth measured downward from sea level. This equation assumes that below some compensation depth the density heterogeneities $\delta\rho$ vanish so that equation (2) remains finite.

In the lithosphere, the total moment M can be divided into a compositional component M_c which relates to the difference between crustal and mantle densities ρ_c and ρ_m, and a thermal moment M_θ

$$M_c = \frac{1}{2}\rho_c g (1 - \frac{\rho_c}{\rho_m}) S^2, \qquad M_\theta = \int_0^{+\infty} z \rho_m g \alpha \theta \, dz, \tag{3}$$

where S is the non uniform crustal thickness, α the thermal expansion coefficient and θ the temperature of the lithosphere minus the deep mantle temperature (i.e. θ and M_θ are negative). Using (3), we make the approximation that the products expansivity times density are the same in the crust and in the lithosphere.

The crustal moment M_c depends on the squared crustal thickness S [England and McKenzie, 1982, 1983]. If the vertical temperature gradient is constant across a thermal lithosphere of thickness L, the thermal moment writes

$$M_\theta = -\frac{1}{3}\rho_m \alpha \Delta\theta g L^2, \tag{4}$$

where $\Delta\theta$ is the temperature increase across the lithosphere. The thermal moment is therefore related to the squared lithospheric thickness.

By isostasy the surface topography h can be expressed in terms of S and L (or in terms of M_c and M_θ using (3)

$$h = \frac{\rho_m - \rho_c}{\rho_m} S - \frac{1}{2}\alpha \Delta\theta L. \tag{5}$$

The lithospheric contribution to isostasy is generally small compared to the crustal contribution.

2.2. Transport

The time-dependence of the crustal moment is obtained by assuming crustal mass conservation:

$$\frac{\partial M_c}{\partial t} + u\frac{\partial M_c}{\partial x} + 2M_c\frac{\partial u}{\partial x} = 0, \tag{6}$$

the coefficient 2 in the last term of the left hand side of (6) comes from the fact that $M_c \propto S^2$ (see (3)). The heat equation multiplied by z and integrated vertically yields the transport of the thermal moment [Lemery et al., 2000]

$$\frac{\partial M_\theta}{\partial t} + u\frac{\partial M_\theta}{\partial x} + 2M_\theta\frac{\partial u}{\partial x} = \kappa\frac{\partial^2 M_\theta}{\partial x^2}, \tag{7}$$

(κ is the thermal diffusivity). The third term of the left hand side expresses the fact that the lithosphere can become thinner by developing cold downwelling instabilities. In equation (7) we have neglected the secular increase in lithospheric thickness due to the difference between

surface cooling (a term which goes as $-\kappa\rho_m g\alpha\Delta\theta$ in Lemery et al. [2000]) and internal radioactive mantle production. In other terms we assume that the planet surface heat flux equals the rate of radiogenic heat production. The secular cooling term is uniform and keeping a modest cooling rate in the equations would not affect our conclusions.

3. Dynamics of the Lithosphere

The dynamics of the lithosphere is therefore controlled at long wavelength by equations (1), (6) and (7). The stability/instability of the crust-lithosphere combination on top of the mantle is akin to that of a light/heavy fluid layer on top of another fluid, namely akin to Rayleigh-Taylor instability. However, due to the thermal diffusive term in the transport equation in (7) but not in (6), the coupled dynamics of the crust and lithosphere yields some surprising behavior with respect to the classical Rayleigh-Taylor instability.

3.1. Stability analysis

In order to solve our system of equations we can replace x,t, u, M_c, M_θ by $L_0\tilde{x}$,$(L_0^2/\kappa)\tilde{t}$, $(\kappa/L_0)\tilde{u}$, $(\eta\kappa/L_0)\tilde{M}_c$, $(\eta\kappa/L_0)\tilde{M}_\theta$ where the $\tilde{}$ variables are now dimensionless. To study the stability of our system, let us assume that the solution consists in a uniform state without any tectonic velocity plus infinitesimal perturbations, $\tilde{M}_c = M_c^0 + \epsilon m_c(x,t)$, $\tilde{M}_\theta = M_\theta^0 + \epsilon m_\theta(x,t)$, $\tilde{u} = \epsilon u(x,t)$, where M_c^0 and M_θ^0 are the uniform dimensionless moments and $\epsilon << 1$. Assuming all terms of order ϵ go as $\exp(ikx + \sigma t)$, our governing equations (1), (6) and (7) yield to first order in ϵ

$$\begin{aligned} 4uk + i(m_c + m_\theta) &= 0, \\ \sigma m_c + 2ikM_c^0 u &= 0, \\ \sigma m_\theta + 2ikM_\theta^0 u + k^2 m_\theta &= 0. \end{aligned} \tag{8}$$

Solving for σ leads to the dispersion relation

$$2\sigma^2 + \sigma(M_\theta^0 + M_c^0 + 2k^2) + k^2 M_c^0 = 0. \tag{9}$$

Depending of the sign of the discriminant of this second degree equation, σ can either be real or imaginary. Let us define k_1 and k_2

$$k_1 = \frac{(\sqrt{|M_\theta^0|} - \sqrt{M_c^0})}{\sqrt{2}}, \quad k_2 = \frac{(\sqrt{|M_\theta^0|} + \sqrt{M_c^0})}{\sqrt{2}}. \tag{10}$$

If $0 < k < |k_1|$ or $k > k_2$, the two roots of the dispersion equation are real and the growth rate σ is

$$\sigma = \frac{1}{2}(k_1 k_2 - k^2) \pm \frac{1}{2}\sqrt{(k_1^2 - k^2)(k_2^2 - k^2)}. \tag{11}$$

On the contrary, when $|k_1| < k < k_2$, the roots are imaginary numbers (i.e. $\sigma = Real(\sigma) + i\omega$),

$$Real(\sigma) = \frac{1}{2}(k_1 k_2 - k^2), \quad \omega = \frac{1}{2}\sqrt{(k^2 - k_1^2)(k_2^2 - k^2)} \tag{12}$$

The roots of the dispersion equation are depicted in Figure 1. When $M_\theta^0 + M_c^0 > 0$ (dotted lines, $k_1 < 0$) the lithosphere is everywhere stable. On the contrary, when $M_\theta^0 + M_c^0 < 0$ (solid lines, $k_1 > 0$) long wavelength perturbations ($k < k_1$) are unstable (the two σ roots are positive). This is the typical case of Rayleigh-Taylor instabilities with a dense fluid on top of a lighter fluid. However, the dynamics are different from the Rayleigh-Taylor situation at shorter wavelengths. For the shortest wavelengths ($k > k_2$), lithospheric thermal anomalies are erased by thermal diffusion and any perturbation vanishes. For $0 < k_1 < k < k_2$, a propagating unstable mode becomes a propagating stable mode as k increases. This tectonic wave propagates as a plane wave at phase velocity ω/k and physically, as it is a dispersive wave, at the group velocity $d\omega/dk$. When $Real(\sigma) = 0$, a pure propagating mode of constant

amplitude exists with wavenumber and angular frequency

$$k_0 = \sqrt{k_1 k_2}, \text{ and } \omega = \frac{1}{2} k_0 (k_2 - k_1). \tag{13}$$

This particular wave propagates with the maximum phase velocity and its group and phase velocities are equal. Its velocity that can easily be expressed in dimensional units by

$$v_p = \frac{1}{2} \sqrt{\frac{\kappa \rho_c (\rho_m - \rho_c) g}{L_0 \eta \rho_m}} S. \tag{14}$$

The existence of a propagating mode is surprising in a context where only diffusive processes occur (diffusion of momentum and diffusion of heat). The propagation occurs while the undulations of the crust and the lithosphere are not in phase. This can be shown by solving (8) which implies that the ratio of the crustal and lithospheric deformations is a complex number,

$$m_\theta = -\frac{m_c}{(k_1 - k_2)^2} \left((k_1^2 + k_2^2 - 2k^2) + 4i\omega \right). \tag{15}$$

We can compare to real geological situations by redimensionalizing our results. The only parameter value whose value is debatable is the lithospheric viscosity. We choose a rather low stiffness of the lithosphere, $L_0 = 50$ km, $\eta = 2\ 10^{21}$ Pa s, which is however the kind of values commonly used to model orogeny [England, 1986; Husson and Ricard, 2004]. The other parameters are standard and yield $k_1 = 0.1$ and $k_2 = 12$ for $S = 40$ km and $L = 83$ km (see parameters in the caption of Figure 2). The compositional and lithospheric moment have opposite signs and similar amplitudes, $M_c^0 = 71$, $M_\theta^0 = -73$. With this parameters, propagation takes place for wavelengths between 26 km and 3140 km. This suggests that much of continental tectonics is either in the unstable regime or in the propagating regime. Only the shortest wavelengths are stable (wavelengths less than 26 km). In this uninteresting domain, however, our long wavelength approximation breaks down.

As seen on Figure 2, the phase and group velocities have typical values from 5 to 10 which in real units corresponds to 3.2 to 6.4 mm yr^{-1}. With the same parameters, $S = 40$ km and $L = 83$ km, propagation at constant amplitude occurs for a wavelength of 287 km and a velocity of 3.7 mm yr^{-1} (see 14).

3.2. Non-Linear Solutions

The previous results have been obtained in the linear stability approximations where the non-linear terms have been neglected. We can also compute the whole non-linear solution using a standard finite difference algorithm with periodic boundary conditions and explicit time-stepping.

In Figure 3, we depicted the solutions for three different cases. The lithospheric thickness has been reduced from (a) to (c) (86, 83 and 80 km thick), so that the dynamics for a wavelength of 1250 km corresponds, unstable, propagating unstable and propagating stable cases, respectively. The initial interfaces are depicted by dashed lines, the final interfaces are depicted by solid lines.

In the case of a thick lithosphere (a), the instability rapidly destabilizes the whole layer and leads to a finite time singularity analog to that discussed in Lemery et al. [2000]. In panels (b) and (c) the propagation to the right of a wave-like deformation is clearly noticeable. The maxima of the lithospheric thickness are shifted to the right with velocities of order 5 mm yr^{-1} in agreement with the marginal stability study. Due to the asymmetry of the lithospheric thickening of panel (b), lithosphere evolves toward what could be interpreted as a series of subduction zones.

The physics of the topography propagation is easy to understand (see Figure 4): the thickness variations of the lithosphere are in advance to those of the crust, in the direction of propagation.

They induced a compression and thus a thickening on the right hand side of the mountain ranges that collapse on their left hand side. Thermal diffusion controls the maximum of the lithospheric thickness and mitigates the overall instability. In the simulations of Figure 3, the difference of phase is difficult to see as it only amounts to about 2^o according to (15).

4. Conclusions

The long wavelength tectonic waves exist when the compositional and thermal moments have somewhat similar amplitudes. This balance is however the typical situation of a mature lithosphere that thickens ($M_\theta + M_c > 0$) until it starts destabilizing ($M_\theta + M_c < 0$). The tectonic wave have velocities given by (14). These velocities are increasing with the average crustal thickness, S and decreasing with the root mean square resistance of the lithosphere, $\sqrt{L_0\eta}$. This traveling mode of tectonics should at any rate be present on Earth or on other planets taking into account the large range of crust and lithosphere thicknesses that can be found.

In orogenic places like Andes and Tibet, the crust is very thick and the lithosphere rather weak, which should signicantly increase the propagation velocity of our tectonic waves. The eastward migration of the compressive front of the Central Andes [Lamb et al., 2001] and the ongoing acceleration of the deformation in the Eastern Cordillera [Kennan, 2000] relate to the emplacement of the cold and dense mantle root evidenced in seismic tomography [Baumont et al., 2002]. In Tibet, the Northeastward developement of the plateau during Tertiary and the accompanying thickening of the lithosphere mantle Tapponnier et al. [2001] can be elegantly explained by the situation described in the panel (b) of Figure 3.

The model is based on a long wavelength analytical model that could be improved to include higher order terms [Medvedev et al., 1999]. It seems however that a natural development of this

study should now use a complete numerical model to take into account the short wavelength deformations and to couple the mechanical lithosphere (here of uniform thickness L_0) to the variable thermal lithosphere.

Acknowledgments. The first author thanks the Yale university where he spends a sabbatical year. The manuscript benefits from discussion with M. Brandon and D. Bercovici and a review by J. Braun. Support was obtained from the CNRS and the Garon Foundation for Supine Geophysics. The second author thanks the M.I.T. for technical support.

References

Argand, E., Comptes-rendus du 13^{eme} Congrès Géologique international, Brussels, 596 pp., 1924.

Artyushkov, E.V., Stresses in the lithosphere caused by crustal thickness inhomogeneities, *J. Geophys. Res., 78*, 7675-7708, 1973.

Baumont , D., A. Paul, G. Zandt, S. Beck, and H. Pedersen, Lithospheric structure of the central Andes based on surface wave dispersion, *J. Geophys. Res., 107*, doi:10.1029/2001JB000345, 2002.

Conrad, C.P., Convective instability of thickening mantle lithosphere, *Geophys. J. Int., 143*, 52-70, 2000.

England, P., and D. McKenzie, A thin viscous sheet model for continental deformation, *Geophys. J. R. Astron. Soc., 70*, 295-321, 1982.

England, P., and D. McKenzie, Correction to: A thin viscous sheet model for continental deformation, *Geophys. J. R. Astron. Soc., 73*, 523-532, 1983.

England, P., Comment on "Brittle failure in the upper mantle during extension of continental lithosphere" by D. Sawyer, *J.Geophys. Res., 91*, 10487-10490, 1986.

Fleitout, L., and C. Froidevaux, Tectonics and topography for lithosphere containing density heterogeneities, *Tectonics, 1*, 21-57, 1982.

Houseman, G.A., D.P. McKenzie, and P. Molnar, Convective instability of a thickened boundary layer and its relevance for the thermal evolution of continental convergent belts, *J. Geophys. Res., 86*, 6115-6132, 1981.

Houseman, G., and P. England, Crustal thickening versus lateral expulsion in the Indian-Asian continental collision, *J. Geophys. Res., 98*, 12,233-12,249, 1993.

Husson, L., and Y. Ricard, Stress balance above subduction zones: application to the Andes, *Earth Planet. Sci. Lett., 222,* 1037-1050, 2004.

Kennan, L., Large-scale geomorphology of the Andes: interrelationships of tectonics, magmatism and climate, in *Geomorphology and global tectonics*, edited by M.A. Summerfield, Wiley, 167-199, 2000.

Lamb, S.H., L. Hoke, and L. Kennan, and J. Dewey, The Cenozoic evolution of the Central Andes in Bolivia and northern Chile, in *Orogens Through Time*, edited by J.P. Burg and M. Ford, Spec. Publ. Geol. Soc. London, 121, 237-264, 1997.

Lémery, C., Y. Ricard, and J. Sommeria, A model for the emergence of thermal plumes in Rayleigh-Bénard convection and infinite Prandtl number, *J. Fluid Mech., 414,* 225-250, 2000.

Medvedev, S., and Y. Podladchikov, New extended thin-sheet approximation for geodynamic applications -I. Model formulation, *Geophys. J. Int., 136*, 567-585, 1999.

Neil, E.A., and G.A. Houseman, Rayleigh-Taylor instability of the upper mantle and its role in intraplate orogeny, *Geophys. J. Int., 138*, 89-107, 1999.

Tapponnier, P., Xu Zhiqin, F. Roger, B. Meyer, N. Arnaud, G. Wittlinger, and Yang Jingsui, Oblique Stepwise Rise and Growth of the Tibet Plateau, *Science 294*, 1671-1677, 2001.

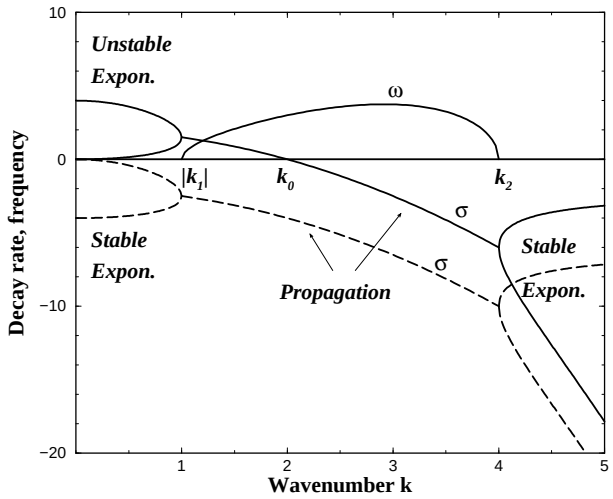

Figure 1. Decay rate σ and angular frequency ω of a perturbation of the crust or the lithospheric thicknesses as a function of the wavenumber k. The solid line corresponds to a case where the lithosphere is globally unstable. As the wavenumber increases, the dynamics shifts from unstable to stable. Between $|k_1|$ and k_2 propagating tectonic waves are excited. The dashed line is for a stable lithosphere. For the clarity of the plot, we used the geologically non relevant values $k_1 = 1$ and $k_2 = 4$ (solid line) and $k_1 = -1$ and $k_2 = 4$ (dashed lines).

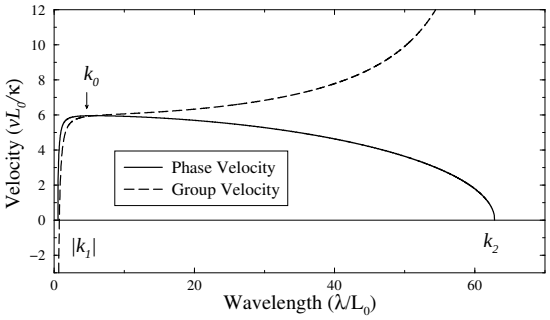

Figure 2. Phase (solid line) and group (dashed line) velocity of a tectonic wave as a function of the normalized wavelength. We use the following parameters: $S = 40$ km, $L = 83$ km, $\eta = 2\ 10^{21}$Pa s, $\kappa = 10^{-6}$m^{2}s^{-1}, $L_0 = 50$ km, $\rho_c = 2800$ kg m^{-3}, $\rho_m = 3200$ kg m^{-3}, $g = 9.8$ m s^{-2}, $\alpha = 3\ 10^{-5}$ K^{-1}, $\theta_m = 1350$ K). With real units, a normalized velocity of 6 corresponds to 3.7 mm yr^{-1}

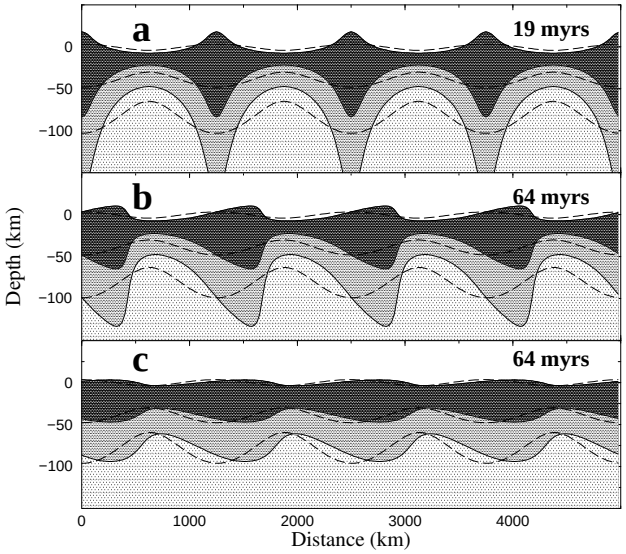

Figure 3. Evolution of the crust and lithosphere with time. The initial sinusoidal interfaces are depicted with dashed lines, the final interfaces with solid lines. The crust, mantle lithosphere and asthenosphere are shaded (darker, intermediate and lighter shades). The initial wavelength is in the domain of unstable ((a) with an initial lithospheric thickness of 86 km), propagating ((b) initial lithospheric thickness of 83 km), and stable ((c) 80 km) regime. For clarity the surface topography has been multiplied by a factor 5. The final solutions have been computed after 19 myrs, (a), and 64 myrs, (b) and (c).

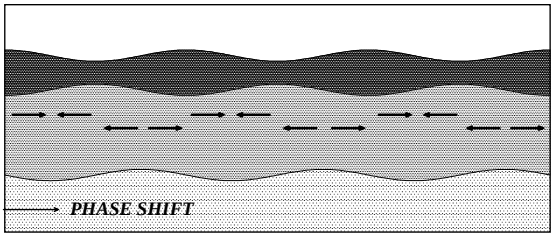

Figure 4. In the propagating mode, the crustal and lithospheric thickening are out of phase, this induces a compression on one side of the mountains, an extension on the other side. This peculiar tectonic setting can then propagate.